Journal of Energy Storage 72 (2023) 108584

Contents lists available at ScienceDirect

Journal of Energy Storage

journal homepage: www.elsevier.com/locate/est

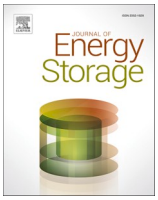

Research papers

Computer-aided design of membrane-free batteries using conductor-like screening model for real solvents

José Pedro Wojeicchowski [a], Catarina S. Neves [a], Paula Navalpotro [b], Rubén Rubio-Presa [c], Edgar Ventosa [c], Rebeca Marcilla [b], João A.P. Coutinho [a,*]

[a] CICECO – Aveiro Institute of Materials, Department of Chemistry, University of Aveiro (UA), 3810-193, Portugal
[b] IMDEA Energy, Electrochemical Processes Unit, Móstoles 28935, Spain
[c] ICCRAM – International Research Centre in Critical Raw Materials, Department of Chemistry, University of Burgos, E-09001, Spain

ARTICLE INFO

Keywords:
Membrane-free RFB
COSMO-RS
Aqueous biphasic system
Methyl viologen
Viologen derivatives

ABSTRACT

The use of renewable energy sources for electricity generation is increasing, and effective energy storage solutions are needed to manage the mismatch between energy production and demand. Redox Flow Batteries (RFBs), particularly Membrane-Free Flow Batteries based on Aqueous Biphasic Systems (ABSs), are a promising technology for stationary energy storage. However, to prevent the crossover of species, the redox-active compounds used in the catholyte and anolyte must be selectively dissolved, which is currently achieved using expensive physical barriers. In this study, an approach was developed to predict the partition coefficient of redox-active compounds in ABSs formed by ionic liquids or polymers, salt, and water using the Conductor-like Screening Model for Real Solvents (COSMO-RS). Experimental data from literature was used to validate the model, resulting in a good correspondence between predicted and experimental data. Furthermore, the method was used to design viologen derivatives and predict their partition coefficients, nine of which were synthesized and validated experimentally. It was found that derivatives containing amine groups have the highest partition coefficients to the salt-rich phase. COSMO-RS proved to be a powerful tool to accelerate the development of advanced biphasic membrane-free flow batteries by designing and finding combinations of redox species with suitable partition coefficients.

1. Introduction

The development of renewable energy sources, namely solar and wind, as alternatives to petroleum, coal, and natural gas, has been increasing to fight global warming and address the energy crisis [1]. In 2021, 22 % of the energy consumed in the European Union (EU) was generated from renewable sources. However, an extensive transformation of the energy system is required to achieve the 2030 EU target of 40 % [2].

The increased integration of the renewable energy sources in the energy system is revealing some limitations such as their inherent intermittency, which can cause mismatches between the production and the demand. To face this drawback, energy storage devices must be coupled to solar or wind farms to store the energy surplus and deliver it when required [3]. Among the various energy storage systems, electrochemical devices stand out due to their efficiency and modularity. In particular, Redox Flow Batteries (RFBs) are suitable candidates for this application since, besides their efficiency, they are the only type of battery able to decouple energy and power densities [4]. The different configuration of these batteries underlies this distinctive feature since in RFB the active species are dissolved into the electrolytes, which are stored in two external tanks and pumped through the cell where the electrochemical reactions take place. In order to avoid the mixing of the electrolytes, the cell is divided into two compartments by an ion selective membrane that allows the movement of ions, keeping the electroneutrality in the cell, and preventing the cross migration of the active species [5]. The most extensively developed and studied RFB is the so called all-vanadium RFB in which the active species are based on vanadium compounds dissolved in acid aqueous solutions and separated by a Nafion membrane [6]. These two components, metallic active species (vanadium based) and Nafion membrane, present some drawbacks which limit the penetration of RFB in the market. In one hand, vanadium is a critical raw material with fluctuating price and limited solubility [7]. On the other hand, the Nafion membranes are poor-

* Corresponding author.
E-mail address: jcoutinho@ua.pt (J.A.P. Coutinho).

https://doi.org/10.1016/j.est.2023.108584
Received 16 May 2023; Received in revised form 25 July 2023; Accepted 31 July 2023

performing and costly (up to 40 % to the overall RFB cost [1,8]). To overcome these issues, the scientific community is making efforts to replace the vanadium compound by more sustainable organic redox materials that can be made out of abundant raw materials, with lower cost and tunable properties by structure functionalization [9–11]. Several families of organic materials have been studied such as TEMPO (nitroxides) [12] ferrocene derivatives [13], phenazines [14], quinones [15,16] or viologens [17]. In the case of Aqueous Redox Flow Batteries (ARFB) at neutral pH, intensive research is being carried out in paring TEMPO derivatives as active species for the catholyte with viologen derivatives for the anolyte [18–23]. Viologens have been studied as suitable anolytes due to their high solubility in water, good electrochemical performance such as fast kinetics, low redox potential and the possibility to exchange two electrons [24]. However, they are prone to suffer parasitic reactions such as re-oxidation with oxygen or dimerization as well as poor solubility in its fully reduced state [24]. Thus, enormous efforts have been made on the functionalization of the viologen structure aiming to increase its solubility, stability, and getting access to the second electron reaction [25,26].

Concurrently, different strategies have been pursued to replace the ion-selective membranes by cheaper porous size-exclusion separators, such as the use of large size soluble redox active polymers [27] or semisolid electrolytes [28,29]. A more radical approach is the complete removal of any membrane or separator by using immiscible/biphasic electrolytes [30,31]. In this regard, Membrane-Free Batteries based on Aqueous Biphasic Systems (ABSs) appeared as disruptive feasible alternatives introduced by Marcilla and co-workers [32–34]. ABSs consist of an aqueous solution of two solutes (salts, ionic liquids or polymers) that above a given concentration spontaneously form two liquid phases [35]. In this innovative concept, ABSs are used as immiscible electrolytes and the redox organic molecules are enriched in each aqueous phase, so that they are kept separated, one in each electrolyte/phase by thermodynamics instead of using a physical separator. This specific solubility is a key factor, since the concentration of active species in the electrolytes will determine the energy density of the battery. Additionally, to avoid capacity losses, a membrane-free battery requires a highly selective separation of different redox molecules (one in the catholyte and the other in the anolyte). Hence, the partition coefficient (*K*) of the redox species should be as different as possible with each redox compound having affinity for a different phase.

The experimental determination of the partition coefficients of ions and organic molecules is costly and lengthy [36,37], in particular if a large number of systems must be scanned to find the most suitable candidates for RFB design. The use of thermodynamic models to predict *K* could be a suitable way for a fast evaluation of the partition coefficients, selecting the most promising systems and designing the modifications that could enhance the partitions and selectivity. COSMO-RS (Conductor-like Screening Model for Real Solvents), which is a predictive thermodynamic model based on quantum chemistry, could be applied for an *in silico* screening of partition coefficients in biphasic systems. It uses atom specific parameters to predict several thermodynamic properties derived from chemical potential, such as activity coefficient [38], phase equilibria [39] and partition coefficients [36,40].

This work aims to evaluate the potential of COSMO-RS in designing redox-active compounds and predicting their partition coefficients in aqueous biphasic systems suitable for the design of aqueous membrane-free batteries. The first part of this work involves evaluating and validating the ability of COSMO-RS to predict the partition coefficients of active redox species using literature data for both polymer-salt and IL-salt ABS.

The compound identified as limiting the selectivity of the redox species, due to its insufficient hydrophilic character is methyl viologen (MV) dichloride. Therefore, COSMO-RS is applied to assess viologen-derivatives to enhance their partition towards the ABS salt-rich phase. Then, nine of these compounds were synthesized, and their partition coefficients measured and compared with COSMO-RS predictions. This process leads to the establishment of fundamental rules for the design of viologen-derivatives.

2. Materials and methods

2.1. Reagents

The ammonium sulfate anhydrous $(NH_4)_2SO_4$, sodium sulfate anhydrous (Na_2SO_4), poly(ethylene glycol) dimethyl ether 250 and 500 g/mol (PEGDME250 and PEGDME500), methyl viologen (MV) dichloride hydrate, 2,2,6,6-tetramethylpiperidine-1-oxyl radical (TEMPO) were purchased from Sigma. The ionic liquid tributyltetradecylphosphonium chloride ($[P_{44414}]Cl$) was supplied by Iolitec. Moreover, several viologen derivatives with different functional groups were synthesized in this work for further evaluation as redox active candidates. Viologens can be synthesized properly by mono- or di-*N*-alkylation of 4,4′-bipyridine with the corresponding alkylating agent, except in the case of viologen F-Br, which was obtained from viologen E-Br by acid hydrolysis of the esters to afford the carboxylic acid terminal groups (Supporting information 1) [25,41–45].

2.2. ABS characterization

The phase diagram of the ternary system composed of polymer or ionic liquid, salt and water was determined gravimetrically ($\pm 10^{-4}$ g) by cloud-point titration method at room temperature (298 ± 1 K), described elsewhere [46]. Briefly, the salt-aqueous solution (40 %) is added dropwise into the neat polymer (or 80 % aqueous solution of IL) until turn it cloud (biphasic region), and then water is drop-added until the system gets back to the monophasic region (limpid solution). This is repeated until no cloud solution is obtained.

The experimental binodal data were fitted using the following Eq. (1) [47]:

$$[Polymer] = Aexp\left[\left(B\,[salt\ or\ IL]^{0.5}\right) - \left(C\,[salt\ or\ IL]^{3}\right)\right] \quad (1)$$

where [Polymer] and [salt or IL] are the mass fraction percentages of those compounds, and the coefficients A, B and C are fitting parameters.

For the tie-line (TL) determination, which represents the final concentration of phase components in the top and bottom phases, the mixture of polymer or IL, salt and water was gravimetrically prepared. After the separation of the phases at 298 ± 1 K overnight, top and bottom phases were individually collected and weighted. Then, the TL was calculated solving the set of the following 4 equations system (Eqs. (2)–(5)). The compositions of the top and bottom phase were determined by the lever-arm rule.

$$[Polymer]_T = Aexp\left[\left(B\,[salt\ or\ IL]_T^{0.5}\right) - \left(C\,[salt\ or\ IL]_T^{3}\right)\right] \quad (2)$$

$$[Polymer]_B = Aexp\left[\left(B\,[salt\ or\ IL]_B^{0.5}\right) - \left(C\,[salt\ or\ IL]_B^{3}\right)\right] \quad (3)$$

$$[Polymer]_T = \frac{[Polymer]_M}{\alpha} - \frac{1-\alpha}{\alpha}[Polymer]_B \quad (4)$$

$$[salt\ or\ IL]_T = \frac{[salt\ or\ IL]_M}{\alpha} - \frac{1-\alpha}{\alpha}[salt\ or\ IL]_B \quad (5)$$

where the subscripts T, B and M are the top phase, the bottom phase and the mixture point, respectively, and α is the mass ratio between the top phase and the total mixture.

2.3. Partition coefficients determination

The partition coefficient (*K*) of the active molecules (MV dichloride, TEMPO and viologen derivatives) was calculated by Eq. (6), which indicates the concentration of the target compound in the different phases

Table 1
Experimental (exp) and predicted (pred) log partition coefficients of each redox compound in the two immiscible phases of several ABS.

Systems	Salt	IL/Pol + Salt + H_2O	TEMPO		MV dichloride		H2Q		AQ2S		QUI		Reference
			exp	pred	exp	pred	exp	pred	exp	pred	exp	pred	
1	Na_2SO_4	$[C_4mim][CF_3SO_3]$	−2.444	−1.417	0.461	0.244	−0.678	−0.871	−1.699	−1.034	−0.854	−1.242	[32]
2		$[C4mim][N(CN)_2]$	0.551	1.338	−0.143	−0.968	1.131	1.025	1.995	0.979	1.060	1.207	
3		$[P_{44414}]Cl$	0.816	1.663	−1.699	−2.429	0.530	1.132	1.119	0.616	1.013	1.192	
4		$[P_{4444}]Br$	1.925	1.456	−1.046	−2.434	1.217	1.243	1.229	1.088	2.355	1.111	
5		$[N_{4444}]Br$	1.747	1.564	−0.886	−1.644	0.607	1.133	1.094	1.260	2.079	1.207	
6		$[P_{4444}][CF_3CO_2]$	0.598	2.457	−2.276	−1.772	0.318	0.753	1.413	3.592	2.268	1.889	
7		PEG1000	0.976	1.295	−0.745	−1.992							[33]
8	$(NH_4)_2SO_4$	PEG1000	2.377[a]	2.378	−1.097	−1.849							[34]
9		PEGDME250	1.910	2.445	−1.685	−2.407							This work
10		PEGDME500	1.954	2.129	−1.886	−2.561							
	r-Value		0.88										

[a] Measured in this work at the same mixture point described in the reference [34].

in equilibrium:

$$K = \frac{[target\ compound]_{top}}{[target\ compound]_{bottom}} \quad (6)$$

For that purpose, the ABS containing electrochemically active molecule was prepared and kept for phase separation overnight at 298 ± 1 K. After that, top and bottom phases were collected and analyzed using spectrophotometry. For viologen derivatives a UV-VIS reader (UV-VIS LAMBDA 1050, Perkin Elmer), in a wavelength range of 200–300 nm was used, and for the systems with MV dichloride and TEMPO, a microplate reader (Synergy|HT, BioTek) was applied, at 260 and 240 nm respectively.

2.4. COSMO-RS simulations

In this work, the COSMO-BP-TZVPD-FINE template of TmoleX software package (interface of TURBOMOLE) [48] was used. It includes a def-TZVPD basis set, DFT with the B-P86 functional level of theory, and the COSMO solvation model (infinite permittivity). This method uses a fine grid which creates a COSMO surface whose segments are more uniform and evenly distributed compared to the standard COSMO cavity. Despite being somewhat more time-consuming, BP-TZVPD-FINE parametrization is considered to be the "best quality" calculation method available up to now on COSMOtherm [49]. After the optimization, the output files, identified by the extension ".cosmo" and available as Supporting information to this article for the active species, are used in the COSMOtherm software [50] for thermodynamic calculations, using the parameterization BP_TZVPD_FINE_21 at 298 K. For the *in silico* estimation of partition coefficient (*K*) it is necessary define the concentration of phases 1 and 2. COSMO-RS assesses the partition coefficients from the chemical potentials according to Eq. (7).

$$log_{10}\left(K_j^{(2,1)}\right) = \frac{\left(\mu_j^{(1)} - \mu_j^{(2)}\right)}{RTln(10)} + log_{10}(VQ) \quad (7)$$

where, VQ is the solvent phase volume quotient, which is estimated from solvent densities ρ_1 and ρ_2.

3. Results and discussion

3.1. Method validation for partition coefficients prediction

Ionic liquids and polymers are widely applied in ABSs for separation, purification and extraction process, as well as in total aqueous membrane-free batteries [33]. They have been increasingly studied as electrolytes in redox-flow batteries due to their unique properties such as thermal and chemical stability, low volatility and high ion conductivity [51,52]. Furthermore, they can be tailored by adjusting their chemical structure to optimize their performance for specific redox-active species, making them a promising candidate for the next generation of redox-flow batteries [52]. Moreover, IL-based ABS can be applied to develop membrane-free batteries that exhibit excellent electrochemical performance and minimal cross contamination [32]. In its turn, polymer-salt ABSs have been extensively researched for extractive separation in ABSs, due to their low cost and environmental benefits [53]. PEG-based ABSs with sodium sulfate [33], and ammonium sulfate [34], as well as PEGDME-based ABSs with ammonium sulfate [54,55] were proven to be suitable platforms for developing batteries.

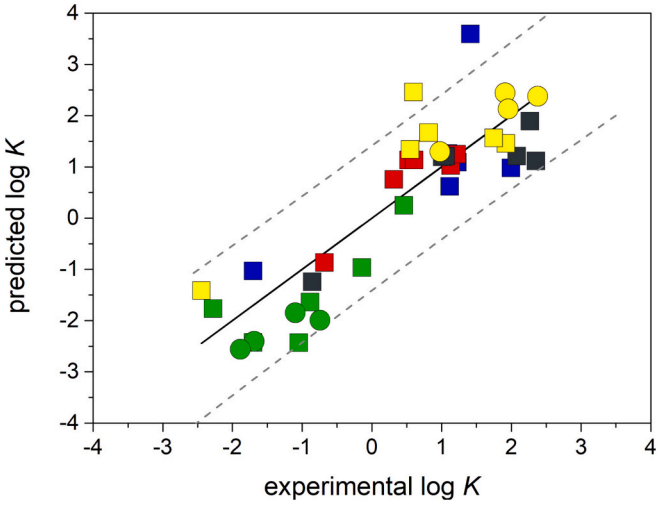

Fig. 1. Predicted *versus* experimental partition coefficient values of redox compounds (AQ2S: blue, H2Q: red, MV dichloride: green, QUI: black, and TEMPO: yellow) in different ABS (squares: ILs, circles: polymers). Perfect prediction (full line) and, 95 % prediction intervals (dashed lines). (For interpretation of the references to color in this figure legend, the reader is referred to the web version of this article.)

The capability of COSMO-RS to predict partition coefficients was assessed by comparing the *K* values of various organic redox molecules in different ABSs against experimental values reported in previous studies [32–34] and complemented, in some cases, with data obtained in this work. The redox compounds used in this analysis included TEMPO, MV dichloride, AQ2S (anthraquinone 2-sulfonic acid sodium salt), H2Q (hydroquinone) and QUI (quinoxaline), which were partitioned in ABS composed of 1-butyl-3-methlimidazolium dicyanamide ($[C_4mim][N(CN)_2]$), 1-butyl-3-methlimidazolium triflate ($[C_4mim][CF_3SO_3]$), tetrabutylammonium bromide ($[N_{4444}]Br$), $[P_{44414}]Cl$, and Poly (ethylene glycol) PEG 1000, combined with sodium sulfate and water. Moreover, ABSs formed by PEG 1000, PEGDME 250 and PEGDME 500, in combination with ammonium sulfate and water, were also evaluated. The database used is presented in Table 1.

Table 2
Names and structures of viologen derivatives designed *in silico*.

Viologen derivatives		
A	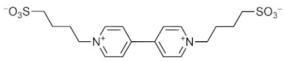	
B	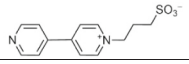	
Viologen derivatives	Cl^-	Br^-
C	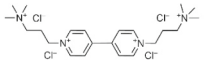	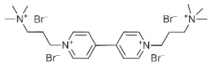
D	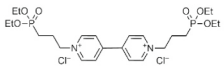	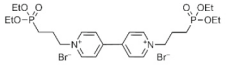
E	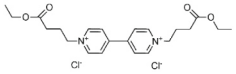	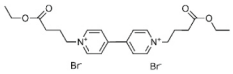
F	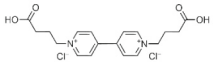	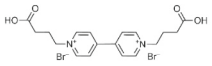
G	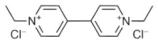	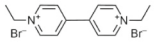
H	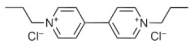	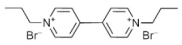
I	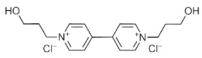	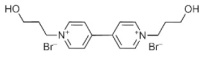
J	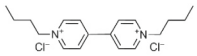	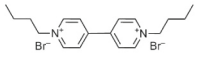
K	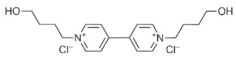	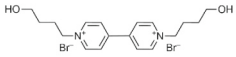
L	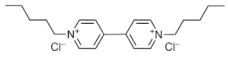	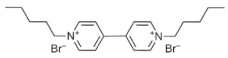
M	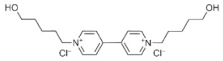	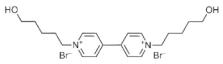
N	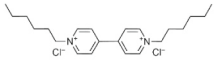	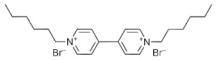
O	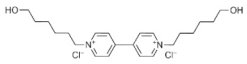	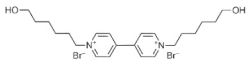
MV	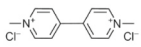	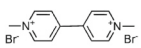

In order to carry out the calculation of partition coefficients using COSMO-RS, the composition of the two phases in equilibrium is required. Tie lines for ILs and PEG1000-based ABS are available in the literature [32–34]. However, for ABSs formed by PEGDME250 and PEGDME500 with ammonium sulfate, phase diagrams were obtained (Fig. S1 and Table S1, Supporting information 2) and a tie line was prepared using a mixture composition of 33 % polymer, 15 % $(NH_4)_2SO_4$ and 52 % water. The phase compositions of each system were obtained by solving Eqs. (1)–(5), and these data were used for *K* prediction (Tables S2 and S3, Supporting information 2).

The partition behavior of the redox compounds is depicted in Fig. 1, where the predicted log K values are plotted against the experimental log K values. The experimental data presented in Table 1 and Fig. 1 show that MV dichloride preferentially partitions to the salt-rich phase, whereas all the other compounds preferentially partition to the IL/polymer-rich phase. The results in Fig. 1 show that the experimental and predicted values follow the same trend, and that, except for two outliers, predicted values fall within the 95 % uncertainty prediction interval, indicating a good agreement between the experimental and predicted values. This observation is further supported by the high Pearson correlation coefficient of 0.87.

Moreover, Fig. S2 from the Supporting information 2 organizes the results by ABSs and demonstrates that the proposed approach based on COSMO-RS is effective in estimating the partition of redox compounds in both IL-based and polymer-based ABS. Overall, the results suggest that the approach used in this study can be helpful to predict and understand the partition of redox compounds in different ABS systems, specially in a qualitative way.

Table 3
COSMO-RS predicted logarithm of partition coefficients (log *K*) of designed viologen derivatives in different ABS.

Viologen derivatives	PEGDME250	PEGDME500	$P_{44414}Cl$			
Viologen A	-1.470		-1.896		-1.676	
Viologen B	0.593		0.210		-0.340	
	Cl			Br		
Viologen derivatives	PEGDME250	PEGDME500	$[P_{44414}]Cl$	PEGDME250	PEGDME500	$[P_{44414}]Cl$
Viologen C	-2.61	-2.51	-3.23	-2.56	-2.90	-3.01
Viologen D	-1.51	-1.73	-1.48	-0.58	-0.14	-0.91
Viologen E	-0.52	0.28	0.68	-0.92	0.87	-0.28
Viologen F	-1.96	-1.99	-1.46	-2.53	-1.18	-1.36
Viologen G	-2.36	-1.69	-0.96	-1.67	-0.79	-0.79
Viologen H	-1.49	-1.33	-1.39	-0.69	-0.87	-0.52
Viologen I	-3.15	-3.09	-2.68	-1.39	-1.51	-2.02
Viologen J	-0.24	-0.27	-0.04	0.46	0.21	0.61
Viologen K'	-1.52	-1.52	-1.71	-0.84	-1.06	-1.16
Viologen L	0.75	0.67	0.91	1.52	1.20	1.61
Viologen M	-0.67	-0.74	-0.94	0.05	-0.25	-0.34
Viologen N	1.75	1.61	1.84	2.54	2.12	2.51
Viologen O	0.32	0.18	-0.03	0.99	0.61	0.55
MV	-1.42	-1.41	-1.79	-1.19	-1.12	-1.56

3.2. Evaluating COSMO-RS in the description of K for viologen derivatives

Viologen species have emerged as promising anolytes in aqueous redox flow batteries [25], along with quinones [32] and phenazines [14]. Their redox potential, solubility and stability can be tailored by the functionalization of their chemical structure. To maximize the battery performance, redox compounds should be partitioned between the ABS phases, with minimal cross contamination. Considering the observed preferential partition of the MV dichloride to the salt-rich phase, that phase will act as the anolyte of our membrane-free battery. Therefore, new viologen derivatives should be highly concentrated in this phase having a chemical structure that maximizes the affinity to the hydrophilic ABS's phase. While MV dichloride partitions preferentially to the salt rich phase, its partition coefficients of log K > -2, is not sufficient to avoid cross contamination. Thus, its partition to the salt-rich phase should be even more extensive.

To find viologen derivatives that showed a higher affinity to the salt-rich phases of the ABS than the MV, 28 viologen derivatives were designed *in silico* (Table 2) for their evaluation by COSMO-RS. The most interesting candidates were selected for experimental validation based on their partition performance and practical limitation associated with their synthesis. Starting from MV, various modifications were introduced in the molecule, including changes in the length of the side chain, and the addition of amine, hydroxyl, carboxyl, ester, phosphoryl and sulfonyl groups. Moreover, the effect of counterions chloride and bromide, was also evaluated, except for derivatives A and B, which are zwitterions and thus do not require counterions. To identify Viologen derivatives (excluding compounds A and B), the following naming convention will be used: Viologen "Letter" - x, where x refers to the counterion (either chloride or bromide). For example, Viologen C-Cl indicates the derivative of Viologen C with chloride as the counterion.

The *K* values for the 28 proposed viologen derivatives were predicted in 3 different systems at the same mixture point: 30%wt of IL ($P_{44414}Cl$) or polymer (PEGDME 250 or PEGDME 500), 20%wt of $(NH_4)_2SO_4$, and 50%wt of water. This mixture point was chosen considering the distance from the binodal curves to ensure that the phases are significantly different and stable.

The color scale in Table 3 represents the qualitative partitioning of viologens, with the highest affinity to the salt-rich phase indicated by the reddest color, while the higher affinity to the polymer/IL phase is indicated by the greenest color. Results from Table 3 revealed that when considering zwitterionic compounds, viologen A showed better partition results compared to derivative B. This can be attributed to the molecular structure of the two compounds. While molecule B has only one pronounced polar area from the sulfonyl group, viologen A has two sulfonyl groups that further increase its polarity. As a result, viologen A has a greater affinity for the hydrophilic phase, which accounts for its superior partition results. Table 3 also showed that, in general, systems with chloride as counter ion had lower (more negative) *K* values, thus more extensive partition to the salt-rich phase, due to the higher electronegativity of chlorine relative to bromine. Moreover, the lengthening of the side chains in the molecules lead, as expected, to increasing hydrophobicity and decreasing the partition of MV. For instance, derivative G had a log *K* of −2.36, whereas incorporating three carbons into each side chain (derivative L) led to a log *K* value of 0.75.

The presence of hydroxyl groups (-OH) in viologen I, led to a significant improvement in log *K* compared to viologen H, which has methyl group instead of -OH. Similar trends were observed in viologens J, L and N, compared to K′, M and O, however, the lengthening of the side chains reduced their affinity to the hydrophilic phase.

Viologen F contains carboxyl groups, which are highly polar and increase the hydrophilicity of the molecule, as indicated by a negative log *K* value. The carboxyl functional group consists of a carbon atom double-bonded to an electronegative oxygen and single-bonded to a hydroxyl (-OH) group, which results in a high polarity. In contrast, viologen E contains ester groups, which are derivatives of carboxylic acids and exhibit lower polarity than carboxyl groups. Esters are slightly soluble in water because they lack a hydrogen atom that can form hydrogen bonds with oxygen atoms. This lower water solubility explains the lower partition of viologen E compared to viologen F, which has two carboxyl groups and is more hydrophilic. In summary, the presence of carboxyl groups in viologen F makes it more water-soluble and polar than viologen E, which has ester groups instead.

Viologens C and D have similar structures, with the only difference being their terminal groups. Viologen C contains amine groups, while viologen D has phosphoryl groups. The presence of amine groups in viologen C enhances its affinity to the salt-rich phase, as evidenced by its log *K* value, $\ll 0$. It is important to note that the polarity of the ABS component, which consists of polymers and ionic liquids, also affects anolyte partition. When the same salt is used, a higher hydrophobicity of the ABS component corresponds to more negative log *K* values, indicating a greater affinity to the salt-rich phase. Therefore, both the terminal groups of viologens C and D and the polarity of the ABS component play a crucial role in determining the partition behavior of the system.

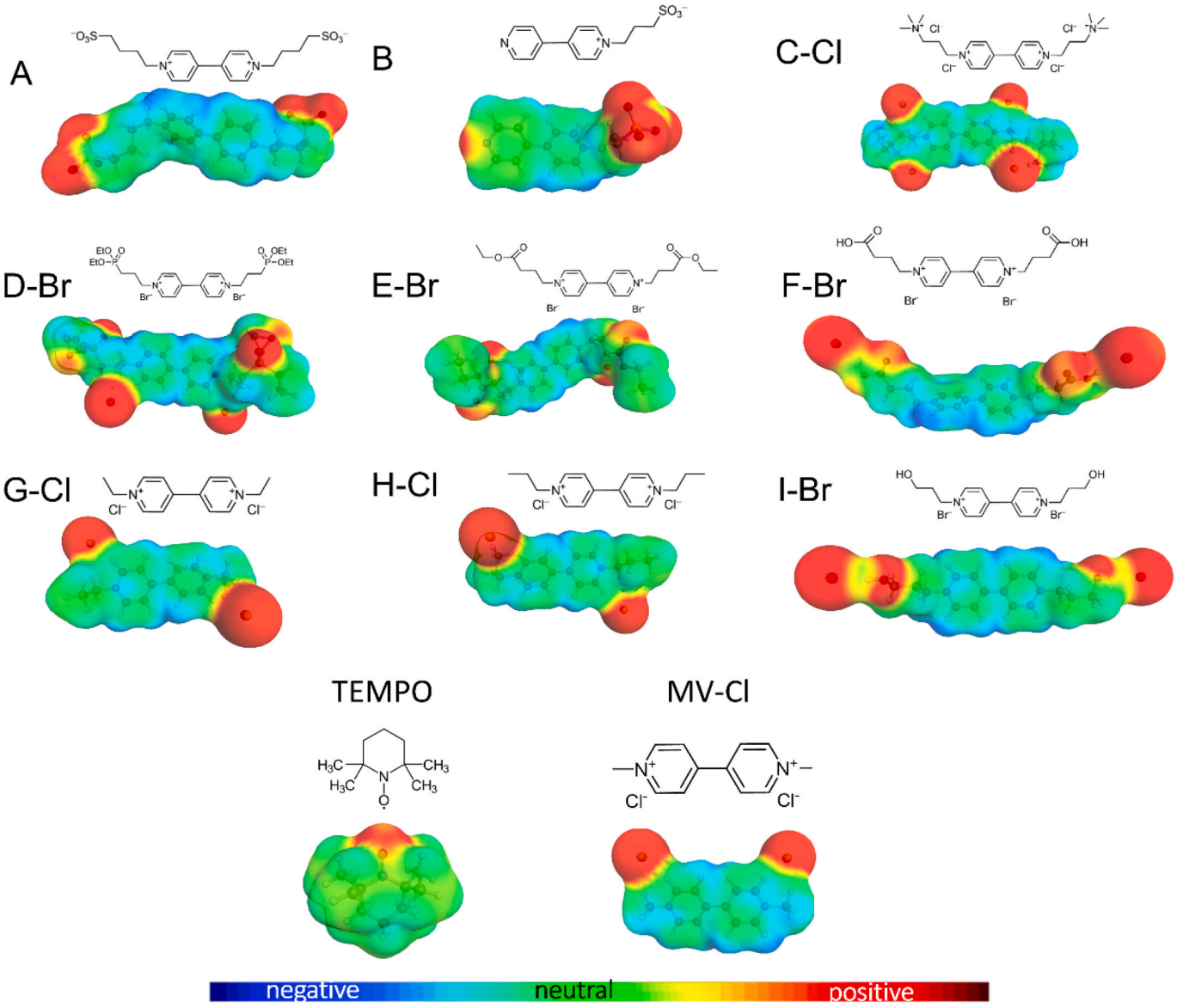

Fig. 2. 2D and 3D representative images of the viologen derivatives synthesized in this work, plus TEMPO and MV dichloride.

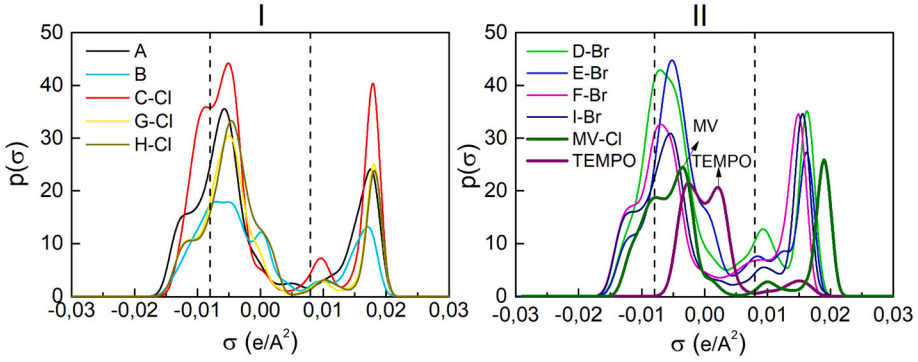

Fig. 3. Sigma-profiles of based redox species: I: (A,B,C-Cl, G-Cl and H-Cl) and II: (D-Br, *E*-Br, F-Br, I-Br, MV-Cl and TEMPO).

Based on the results presented in Table 3 and considering technical aspects and limitations imposed by the synthesis, 9 viologen derivatives, shown in Fig. 2, were synthesized for further *K* evaluation. Fig. 2 displays the minimum energy conformations of each molecule, which represent their most stable structures. The surfaces of the molecules are color-coded to distinguish their negative and positive polar regions, which are depicted in deep red and deep blue, respectively. Weakly polar or non-polar regions are colored green, with blue-green indicating

Table 4
Experimental and COSMO-RS predicted log of partition coefficients (log *K*) of the synthesized viologen derivatives and MV dichloride in different ABS at the mixture point: 30%wt Polymer/IL + 20%wt $(NH_4)_2SO4$ + 50%wt water and their estimated polarity.

Compounds	% Polarity of compounds	System 1: PEGDME250		System 2: PEGDME500		System 3: $[P_{44414}]Cl$	
		exp	pred	exp	pred	exp	pred
A	54	−1.991 ± 0.01	−1.470	−1.004 ± 0.01	−1.432	−0.394 ± 0.01	−1.274
B	48	0.423 ± 0.01	0.593	0.331 ± 0.05	0.210	−0.353 ± 0.04	−0.340
C-Cl	57	−3.222 ± 0.02	−2.608	−2.276 ± 0.08	−2.508	−2.260 ± 0.01	−3.227
D-Br	49	−0.534 ± 0.09	−0.578	0.036 ± 0.07	−0.137	−0.924 ± 0.02	−0.909
E-Br	40	−0.709 ± 0.07	−0.919	0.717 ± 0.01	0.870	−0.321 ± 0.01	−0.279
F-Br	58	−2.481 ± 0.01	−2.535	−1.405 ± 0.01	−1.179	−1.338 ± 0.01	−1.362
G-Cl	46	−2.796 ± 0.03	−2.362	−1.575 ± 0.01	−1.695	−0.995 ± 0.04	−0.958
H-Cl	41	−2.180 ± 0.01	−1.488	−0.437 ± 0.05	−1.331	−1.402 ± 0.01	−1.394
I-Br	55	−1.538 ± 0.01	−1.386	−1.622 ± 0.01	−1.513	−2.056 ± 0.01	−2.019
MV-Cl	51	−1.544 ± 0.08	−1.416	−1.585 ± 0.08	−1.405	−1.856 ± 0.09	−1.792
r-Value		0.97		0.95		0.89	

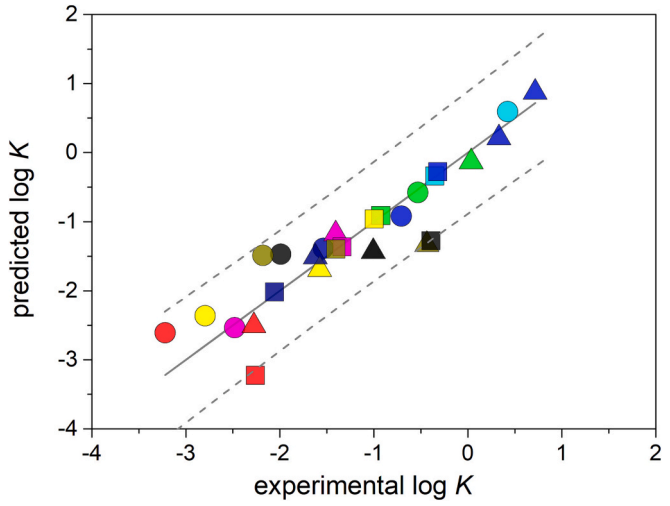

Fig. 4. Predicted *versus* experimental partition coefficient values of viologen derivatives (A: black, B: cyan, C-Cl: red, D-Br: green, E-Br: blue, F-Br: magenta, G-Cl: yellow, H-Cl: dark yellow, and, I-Br: navy blue) in different ABS: PEGDME250: circles, PEGDME500: triangles, $[P_{44414}]Cl$: squares, with $(NH_4)_2SO_4$ and water Perfect prediction (full line) and, 95 % prediction intervals (dashed lines). (For interpretation of the references to color in this figure legend, the reader is referred to the web version of this article.)

hydrogen areas and yellow-green representing carbon regions. Therefore, a simple and generic rule can be inferred from the color scheme: the more colorful the molecule, the higher its polarity.

The Fig. 2 provides the full 3D information on the molecular surface charge and can be represented by a molecule fingerprint called the sigma-profile (σ-profile). Fig. 3 presents the σ-profile -for the 9 selected viologen-derivatives plus TEMPO and MV dichloride. These are histograms, denoted as $p^X(\sigma)$ that show the proportion of the molecule's surface that belongs to a specific polarity interval. It is important to note that due to the sign inversion of the polarization charge density, σ, relative to molecular polarity, the peak from the negative lone pairs is located on the right side of the σ-profile, while the peak arising from positively polar hydrogens is located on the left side [56].

Fig. 3 shows that anolytes have peaks beyond the hydrogen bond (hb) threshold $\pm\sigma_{hb} = \pm 0.082\ e/A^2$, specially in the positive region, *i.e.* showing a high hydrogen bond acceptor ability. Another characteristic of anolyte profiles is their notable asymmetry with respect to σ. There is an imbalance between the strongly positive and strongly negative surface areas, which do not allow for energetically favorable pairings of positive and negative surfaces to form strong hydrogen bonds without additional partners. In contrast, the catholyte TEMPO, in Fig. 3 II, is predominantly non-polar, with most of its surface area falling within the range of $\pm\sigma_{hb} = 0.01\ e/A^2$. Note that TEMPO's curve exhibits a small peak at around $+0.015\ e/A^2$, which arises from the exposed surfaces of their carbon atoms. The σ-profile analysis reveals that the catholyte (TEMPO) and anolytes have distinct polarities, which will influence their partition in ABSs. Specifically, viologen derivatives selected will preferentially partition into the hydrophilic phase, while TEMPO, as shown before, partitions into the hydrophobic phase.

The partition behavior of the 9 viologen derivatives shown in Fig. 2 were evaluated for the ABSs composed of 30%wt of IL ($P_{44414}Cl$) or polymer (PEGDME 250 or PEGDME 500), 20%wt of $(NH_4)_2SO_4$, and 50%wt of water. Table 4 presents the experimental and predicted log *K*, and contains the values of viologen polarity, while Fig. 4 illustrates the partition results graphically. Overall, the results demonstrate that COSMO-RS accurately predicted the partition behavior of viologen derivatives in various ABSs, as depicted in Fig. 4, with Pearson correlation equal to 0.92. Further details and discussion are available in Supporting information 2, Figs. S3–S8. Table 4 shows the polarity order of the different viologen derivatives, with viologen F-Br being the most polar, followed C-Cl, I-Br, A, MV-Cl, D-Br, B, G-Cl, H-Cl, and *E*-Br, in descending order of polarity. The overall polarity of MV derivatives was calculated by integrating the σ-profile curves under the polar region, which was defined as the peaks beyond the hb threshold $\pm\sigma_{hb} = \pm 0.082\ e/A^2$ [57], in comparison to the integral of the entire σ-profile (Fig. S9, Supporting information 2). It was observed that the addition of methyl groups, as seen in derivatives G-Cl and H-Cl compared to MV, increased their hydrophobicity, which decreased their affinity to the salt-rich phase. Viologen E-Br, in turn, exhibited the lowest polarity among all the derivatives due to its larger side chain compared to MV, combined with the presence of ester groups, which have low ability to form intermolecular hydrogen bonding. On the other hand, the polarity scale showed that derivatives F-Br, C-Cl, I-Br and A had higher polarity than MV-Cl. In general, these derivatives displayed a greater hydrophilic behavior than to MV-Cl. For instance, viologen C-Cl had log $K < -2$ in all the systems indicating a good affinity to the salt-rich phase minimizing cross contamination with the catholyte. As discussed earlier, the structure of viologen derivatives has a significant impact on their polarity which, in turn, affects how anolytes were distributed between the phases of ABSs. But the partition behavior of viologens is not driven solely by their structure but is dependent on a combination of the ABS phases composition that impact on how the viologen interacts and partitions between the phases.

The results here reported demonstrate that COSMO-RS can be used in various ways to design systems suitable for use in the preparation of membrane free batteries. It can guide the selection of redox compounds for a particular ABS, and it can also assist in the choice of an ABS for a given redox molecule, or it can be used to evaluate multiple systems and compounds simultaneously, as shown in this work. It is worth noting that the integration of *in silico* design of several viologen derivatives with the ability of COSMO-RS to predict their partition coefficients, helped to

identify promising derivatives, such as C-Cl, I-Br and F-Br, to be applied in aqueous biphasic membrane-free flow batteries.

4. Conclusion

In summary, this work presents a COSMO-RS-based method to predict partition behavior of redox compounds in aqueous biphasic systems for membrane-free battery design. Firstly, the approach was validated using literature data and demonstrated a good correspondence between predicted and experimental results, with a Pearson correlation coefficient (r) equal to 0.88. After that, 28 viologen derivatives were designed *in silico* and their partition was investigated in 3 different ABSs. Results indicated that the redox compounds with higher hydrophilicity had a greater affinity to the salt-rich phase. To understand how the modification in the structure of viologen affects their partition, 9 viologen derivatives were synthesized and tested in the ABSs. According to the calculated polarity, viologens F-Br and C-Cl were the most hydrophilic, due to the presence of carboxyl and amine groups, respectively, while viologen E showed a lower hydrophilic character. Moreover, a high correlation ($r = 0.92$) was obtained between experimental and predicted K for viologen derivatives, which reinforces the predictivity ability of the model. COSMO-RS demonstrates to be a valuable screening tool for help designing redox species candidates and evaluating their partition behavior in a range of aqueous biphasic systems, prior to carrying out costly and time-consuming experimental analyses. Considering the relevance of the partition coefficient in aqueous biphasic membrane-free flow batteries, the proposed computer-aided tool proved to help designing and selecting highly hydrophilic derivatives, such as viologen C-Cl ($\log K < 2$), which may accelerate the development in this emerging field.

CRediT authorship contribution statement

José Pedro Wojeicchowski: Conceptualization, Investigation, Methodology, Data curation, Writing – original draft. **Catarina S. Neves:** Investigation, Methodology, Writing – review & editing, Data curation. **Paula Navalpotro:** Investigation, Writing – review & editing. **Rubén Rubio-Presa:** Investigation, Writing – review & editing. **Edgar Ventosa:** Conceptualization, Funding acquisition, Resources, Writing – review & editing. **Rebeca Marcilla:** Investigation, Writing – review & editing. **João A.P. Coutinho:** Conceptualization, Resources, Supervision, Funding acquisition, Project administration, Writing – review & editing.

Declaration of competing interest

The authors declare that they have no known competing financial interests or personal relationships that could have appeared to influence the work reported in this paper.

Data availability

Files attached at the attach file step in a .zip format.

Acknowledgments

This work was developed within the scope of the project CICECO-Aveiro Institute of Materials, UIDB/50011/2020, UIDP/50011/2020 & LA/P/0006/2020, financed by national funds through the FCT/MCTES (PIDDAC). The authors acknowledge the financial support by the MeBattery project. MeBattery has received funding from the European Innovation Council of the European Union under Grant Agreement no. 101046742.

Appendix A. Supplementary data

Supplementary data to this article can be found online at https://doi.org/10.1016/j.est.2023.108584.

References

[1] X. Wang, A. Lashgari, J. Chai, J. "Jimmy" Jiang, A membrane-free, aqueous/nonaqueous hybrid redox flow battery, Energy Storage Mater. 45 (2022) 1100–1108, https://doi.org/10.1016/J.ENSM.2021.11.008.
[2] European Environment Agency, Progress Towards Renewable Energy Source Targets for EU-27, Copenhagen, 2022.
[3] A.A. Kebede, T. Kalogiannis, J. Van Mierlo, M. Berecibar, A comprehensive review of stationary energy storage devices for large scale renewable energy sources grid integration, Renew. Sust. Energ. Rev. 159 (2022), 112213, https://doi.org/10.1016/J.RSER.2022.112213.
[4] P. Alotto, M. Guarnieri, F. Moro, Redox flow batteries for the storage of renewable energy: a review, Renew. Sust. Energ. Rev. 29 (2014) 325–335, https://doi.org/10.1016/J.RSER.2013.08.001.
[5] H. Zhang, X. Li, J. Zhang, Redox Flow Batteries: Fundamentals and Applications, 2017, https://doi.org/10.1201/9781315152684.
[6] M. Skyllas-Kazacos, Review—highlights of UNSW all-vanadium redox battery development: 1983 to present, J. Electrochem. Soc. 169 (2022), 070513, https://doi.org/10.1149/1945-7111/ac7bab.
[7] International Energy Agency (IEA), Final List of Critical Minerals 2022, 2023.
[8] L. Tang, P. Leung, M.R. Mohamed, Q. Xu, S. Dai, X. Zhu, C. Flox, A.A. Shah, Q. Liao, Capital cost evaluation of conventional and emerging redox flow batteries for grid storage applications, Electrochim. Acta 437 (2023), 141460, https://doi.org/10.1016/J.ELECTACTA.2022.141460.
[9] Z. Li, T. Jiang, M. Ali, C. Wu, W. Chen, Recent progress in organic species for redox flow batteries, Energy Storage Mater. 50 (2022) 105–138, https://doi.org/10.1016/J.ENSM.2022.04.038.
[10] F. Zhong, M. Yang, M. Ding, C. Jia, Organic electroactive molecule-based electrolytes for redox flow batteries: status and challenges of molecular design, Front Chem. 8 (2020), https://doi.org/10.3389/fchem.2020.00451.
[11] W. Wang, V. Sprenkle, Redox flow batteries go organic, Nat. Chem. 8 (2016) 204–206, https://doi.org/10.1038/nchem.2466.
[12] W. Zhou, W. Liu, M. Qin, Z. Chen, J. Xu, J. Cao, J. Li, Fundamental properties of TEMPO-based catholytes for aqueous redox flow batteries: effects of substituent groups and electrolytes on electrochemical properties, solubilities and battery performance, RSC Adv. 10 (2020), https://doi.org/10.1039/d0ra03424j.
[13] J. Luo, M. Hu, W. Wu, B. Yuan, T.L. Liu, Mechanistic insights of cycling stability of ferrocene catholytes in aqueous redox flow batteries†, Energy Environ. Sci. 15 (2022) https://doi.org/10.1039/d1ee03251h.
[14] C. De La Cruz, A. Molina, N. Patil, E. Ventosa, R. Marcilla, A. Mavrandonakis, New insights into phenazine-based organic redox flow batteries by using high-throughput DFT modelling, Sustain Energy Fuels. 4 (2020), https://doi.org/10.1039/d0se00687d.
[15] S. Er, C. Suh, M.P. Marshak, A. Aspuru-Guzik, Computational design of molecules for an all-quinone redox flow battery, Chem. Sci. 6 (2015), https://doi.org/10.1039/c4sc03030c.
[16] P. Symons, Quinones for redox flow batteries, Curr Opin Electrochem. 29 (2021), 100759, https://doi.org/10.1016/j.coelec.2021.100759.
[17] Y. Liu, Y. Li, P. Zuo, Q. Chen, G. Tang, P. Sun, Z. Yang, T. Xu, Screening viologen derivatives for neutral aqueous organic redox flow batteries, ChemSusChem. 13 (2020), https://doi.org/10.1002/cssc.202000381.
[18] T. Liu, X. Wei, Z. Nie, V. Sprenkle, W. Wang, A total organic aqueous redox flow battery employing a low cost and sustainable methyl viologen anolyte and 4-HO-TEMPO catholyte, Adv. Energy Mater. 6 (2016), https://doi.org/10.1002/aenm.201501449.
[19] B. Hu, M. Hu, J. Luo, T.L. Liu, A. Stable, Low permeable TEMPO catholyte for aqueous total organic redox flow batteries, Adv. Energy Mater. 12 (2022), https://doi.org/10.1002/aenm.202102577.
[20] M. Pan, L. Gao, J. Liang, P. Zhang, S. Lu, Y. Lu, J. Ma, Z. Jin, Reversible redox chemistry in pyrrolidinium-based TEMPO radical and extended viologen for high-voltage and long-life aqueous redox flow batteries, Adv. Energy Mater. 12 (2022), https://doi.org/10.1002/aenm.202103478.
[21] T. Janoschka, N. Martin, M.D. Hager, U.S. Schubert, An aqueous redox-flow battery with high capacity and power: the TEMPTMA/MV system, Angewandte Chemie - International Edition. 55 (2016), https://doi.org/10.1002/anie.201606472.
[22] Y. Liu, M.A. Goulet, L. Tong, Y. Liu, Y. Ji, L. Wu, R.G. Gordon, M.J. Aziz, Z. Yang, T. Xu, A long-lifetime all-organic aqueous flow battery utilizing TMAP-TEMPO radical, Chem. 5 (2019), https://doi.org/10.1016/j.chempr.2019.04.021.
[23] H. Fan, W. Wu, M. Ravivarma, H. Li, B. Hu, J. Lei, Y. Feng, X. Sun, J. Song, T.L. Liu, H. Fan, M. Ravivarma, H. Li, J. Lei, Y. Feng, J. Song, W. Wu, T.L. Liu, X. Sun, Mitigating ring-opening to develop stable TEMPO catholytes for pH-neutral all-organic redox flow batteries, Adv. Funct. Mater. 32 (2022) 2203032, https://doi.org/10.1002/ADFM.202203032.
[24] C.L. Bird, A.T. Kuhn, Electrochemistry of the viologens, Chem. Soc. Rev. 10 (1981), https://doi.org/10.1039/CS9811000049.
[25] R. Rubio-Presa, L. Lubián, M. Borlaf, E. Ventosa, R. Sanz, Addressing practical use of viologen-derivatives in redox flow batteries through molecular engineering, ACS Mater. Lett. (2023) 798–802, https://doi.org/10.1021/ACSMATERIALSLETT.2C01105.

[26] Y. Liu, Q. Chen, X. Zhang, J. Ran, X. Han, Z. Yang, T. Xu, Degradation of electrochemical active compounds in aqueous organic redox flow batteries, Curr Opin Electrochem. 32 (2022), https://doi.org/10.1016/j.coelec.2021.100895.
[27] T. Janoschka, N. Martin, U. Martin, C. Friebe, S. Morgenstern, H. Hiller, M. D. Hager, U.S. Schubert, An aqueous, polymer-based redox-flow battery using non-corrosive, safe, and low-cost materials, Nature 527 (2015), https://doi.org/10.1038/nature15746.
[28] E. Ventosa, D. Buchholz, S. Klink, C. Flox, L.G. Chagas, C. Vaalma, W. Schuhmann, S. Passerini, J.R. Morante, Non-aqueous semi-solid flow battery based on Na-ion chemistry. P2-type NaxNi0.22Co0.11Mn0.66O2-NaTi2(PO4)3, Chem. Commun. 51 (2015), https://doi.org/10.1039/c4cc09597a.
[29] Z. Li, K.C. Smith, Y. Dong, N. Baram, F.Y. Fan, J. Xie, P. Limthongkul, W.C. Carter, Y.M. Chiang, Aqueous semi-solid flow cell: demonstration and analysis, Phys. Chem. Chem. Phys. 15 (2013), https://doi.org/10.1039/c3cp53428f.
[30] X. Li, Z. Qin, Y. Deng, Z. Wu, W. Hu, Development and challenges of biphasic membrane-less redox batteries, Advanced Science. 9 (2022) 2105468, https://doi.org/10.1002/advs.202105468.
[31] P. Navalpotro, J. Palma, M. Anderson, R. Marcilla, A membrane-free redox flow battery with two immiscible redox electrolytes, Angewandte Chemie-International Edition. 56 (2017), https://doi.org/10.1002/anie.201704318.
[32] P. Navalpotro, C.M.S.S. Neves, J. Palma, M.G. Freire, J.A.P. Coutinho, R. Marcilla, Pioneering use of ionic liquid-based aqueous biphasic systems as membrane-free batteries, Advanced Science. 5 (2018) 1800576, https://doi.org/10.1002/advs.201800576.
[33] P. Navalpotro, C. Trujillo, I. Montes, C.M.S.S. Neves, J. Palma, M.G. Freire, J.A. P. Coutinho, R. Marcilla, Critical aspects of membrane-free aqueous battery based on two immiscible neutral electrolytes, Energy Storage Mater. 26 (2020) 400–407, https://doi.org/10.1016/J.ENSM.2019.11.011.
[34] P. Navalpotro, S.E. Ibañez, E. Pedraza, R. Marcilla, A neutral pH aqueous biphasic system applied to both static and flow membrane-free battery, Energy Storage Mater. 56 (2023) 403–411, https://doi.org/10.1016/J.ENSM.2023.01.033.
[35] J.F.B. Pereira, M.G. Freire, J.A.P. Coutinho, Aqueous two-phase systems: towards novel and more disruptive applications, Fluid Phase Equilib. 505 (2020), https://doi.org/10.1016/j.fluid.2019.112341.
[36] M. Zawadzki, K. Paduszyński, M. Królikowska, E. Grzechnik, COSMO-RS predicted 1-octanol/water partition coefficient as useful ion descriptor for predicting phase behavior of aqueous solutions of ionic liquids, J. Mol. Liq. 307 (2020), 112914, https://doi.org/10.1016/J.MOLLIQ.2020.112914.
[37] J. Ghasemi, S. Saaidpour, Quantitative structure-property relationship study of n-octanol-water partition coefficients of some of diverse drugs using multiple linear regression, Anal. Chim. Acta 604 (2007), https://doi.org/10.1016/j.aca.2007.10.004.
[38] C. Araya-López, J. Contreras, G. Merlet, R. Cabezas, F. Olea, E. Villarroel, R. Salazar, J. Romero, E. Quijada-Maldonado, [Tf2N]-based ionic liquids for the selective liquid-liquid extraction of levulinic acid/formic acid: COSMO-RS screening and ternary LLE experimental data, Fluid Phase Equilib. 561 (2022), 113518, https://doi.org/10.1016/J.FLUID.2022.113518.
[39] M. Wlazło, E.I. Alevizou, E.C. Voutsas, U. Domańska, Prediction of ionic liquids phase equilibrium with the COSMO-RS model, Fluid Phase Equilib. 424 (2015) 16–31, https://doi.org/10.1016/j.fluid.2015.08.032.
[40] J.-B. Chagnoleau, N. Papaiconomou, M. Jamali, D.O. Abranches, J.A.P. Coutinho, X. Fernandez, T. Michel, Toward a critical evaluation of DES-based organic biphasic systems: are deep eutectic solvents so critical? ACS Sustainable Chemistry & Engineering 9 (2021) 9707–9716, https://doi.org/10.1021/acssuschemeng.1c01628.
[41] E.S. Beh, D. De Porcellinis, R.L. Gracia, K.T. Xia, R.G. Gordon, M.J. Aziz, A neutral pH aqueous organic- organometallic redox flow battery with extremely high capacity retention, ACS Energy Lett. 2 (2017), https://doi.org/10.1021/acsenergylett.7b00019.
[42] M. Felderhoff, S. Heinen, N. Molisho, S. Webersinn, L. Walder, Molecular suppression of the pimerization of viologens (=4,4′-bipyridinium derivatives) attached to nanocrystalline titanium dioxide thin-film electrodes, Helv Chim Acta. 83 (2000) 181–192, https://doi.org/10.1002/(SICI)1522-2675(20000119)83:1<181::AID-HLCA181>3.0.CO;2-U.
[43] Y. Zheng, A.E. Kaifer, Kinetics and thermodynamics of binding between zwitterionic viologen guests and the cucurbit[7]uril host, J. Org. Chem. 85 (2020), https://doi.org/10.1021/acs.joc.0c01201.
[44] K. Moon, A.E. Kaifer, Modes of binding interaction between viologen guests and the cucurbit[7]uril host, Org. Lett. 6 (2004), https://doi.org/10.1021/ol035967x.
[45] W. Ong, M. Gómez-Kaifer, A.E. Kaifer, Cucurbit[7]uril: a very effective host for viologens and their cation radicals, Org. Lett. 4 (2002), https://doi.org/10.1021/ol025869w.
[46] C.M.S.S. Neves, S.P.M. Ventura, M.G. Freire, I.M. Marrucho, J.A.P. Coutinho, Evaluation of cation influence on the formation and extraction capability of ionic-liquid-based aqueous biphasic systems, J. Phys. Chem. B 113 (2009), https://doi.org/10.1021/jp900293v.
[47] J.C. Merchuk, B.A. Andrews, J.A. Asenjo, Aqueous two-phase systems for protein separation studies on phase inversion, J. Chromatogr. B Biomed. Appl. 711 (1998) 285–293, https://doi.org/10.1016/S0378-4347(97)00594-X.
[48] C. Steffen, K. Thomas, U. Huniar, A. Hellweg, O. Rubner, A. Schroer, TmoleX-A graphical user interface for TURBOMOLE, J. Comput. Chem. 31 (2010) 2968–2970, https://doi.org/10.1002/jcc.21576.
[49] COSMOlogic (Ed.), COSMOtherm Reference Manual, 19th ed., Cosmologic, Leverkusen, 2018.
[50] F. Eckert, A. Klamt, Fast solvent screening via quantum chemistry: COSMO-RS approach, AICHE J. 48 (2002) 369–385, https://doi.org/10.1002/AIC.690480220.
[51] S. Seki, S. Ono, N. Serizawa, Y. Umebayashi, S. Tsuzuki, K. Ueno, M. Watanabe, Design and new energy application of ionic liquids, RSC Smart Materials (2018), https://doi.org/10.1039/9781788011839-00365.
[52] V.M. Ortiz-Martínez, L. Gómez-Coma, G. Pérez, A. Ortiz, I. Ortiz, The roles of ionic liquids as new electrolytes in redox flow batteries, Sep. Purif. Technol. 252 (2020), 117436, https://doi.org/10.1016/J.SEPPUR.2020.117436.
[53] N.V. Dos Santos, M. Martins, V.C. Santos-Ebinuma, S.P.M. Ventura, J.A. P. Coutinho, S.R. Valentini, J.F.B. Pereira, Aqueous biphasic systems composed of cholinium chloride and polymers as effective platforms for the purification of recombinant green fluorescent protein, ACS Sustain. Chem. Eng. 6 (2018), https://doi.org/10.1021/acssuschemeng.8b01730.
[54] I. Jeon, W.G. Hong, S. Yoon, Y. Choi, H.J. Kim, J.-P. Kim, Safety, high-performing and effects of the N/P ratio of a solid lithium ion battery using PEGDME based polymer electrolytes, Heliyon 9 (2023), e13292, https://doi.org/10.1016/J.HELIYON.2023.E13292.
[55] L. Carbone, M. Gobet, J. Peng, M. Devany, B. Scrosati, S. Greenbaum, J. Hassoun, Polyethylene glycol dimethyl ether (PEGDME)-based electrolyte for lithium metal battery, J. Power Sources 299 (2015) 460–464, https://doi.org/10.1016/J.JPOWSOUR.2015.08.090.
[56] A. Klamt, COSMO-RS From Quantum Chemistry to Fluid Phase Thermodynamics and Drug Design, 1st ed., Elsevier, Amsterdam, 2005 https://doi.org/10.1016/b978-044451994-8/50000-6.
[57] D.O. Abranches, J. Benfica, B.P. Soares, A. Leal-Duaso, T.E. Sintra, E. Pires, S. P. Pinho, S. Shimizu, J.A.P. Coutinho, Unveiling the mechanism of hydrotropy: evidence for water-mediated aggregation of hydrotropes around the solute, Chem. Commun. 56 (2020), https://doi.org/10.1039/d0cc03217d.